Supplementary Information

Image correlation spectroscopy as a tool for microrheology of soft materials

Nicholas Agung Kurniawan[a], Chwee Teck Lim[a,b,c], Raj Rajagopalan*[a,d,e]
[a] *NUS Graduate School for Integrative Sciences and Engineering, Singapore 117456. E-mail: raj@nus.edu.sg*
[b] *Department of Mechanical Engineering, National University of Singapore, Singapore 117576*
[c] *Division of Bioengineering, National University of Singapore, Singapore 117574*
[d] *Department of Chemical and Biomolecular Engineering, National University of Singapore, Singapore 117576*
e Chemical and Pharmaceutical Engineering Program, Singapore-MIT Alliance National University of Singapore, Singapore 117576

Steps involved in ICS-μR

Here, we present the details of the practical aspects and implementations in the ICS-μR analysis. To help the reader with the various quantities involved in the analysis, Fig. S1 illustrates the calculation stages that will be subsequently discussed.

All symbols and their meanings in this Supplementary Information are the same as those used in the main article, and explanations of the notations are, therefore, not repeated unless necessary.

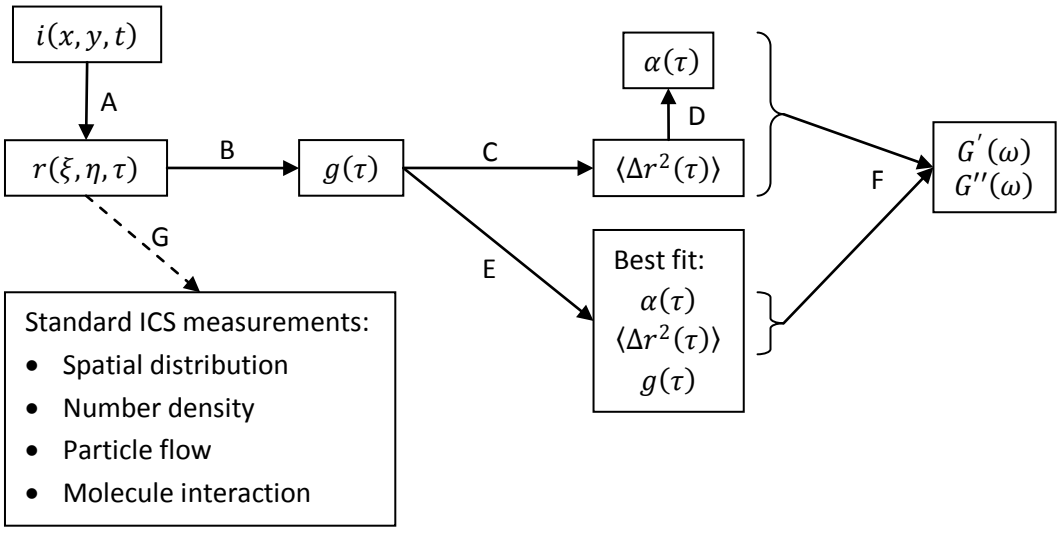

Fig. S1 A schematic overview of data analysis steps involved in ICS-μR. The steps A through F are explained in the text below. Steps A, B, and G are routinely followed in standard ICS measurements, whereas Steps D and F are routinely used in standard microrheology measurements. In the present work, we introduce Step C, which allows microrheological analysis from ICS data, as well as Step E, which improves the quality of the microrheological results extracted from the data.

Step A

The raw data for ICS is a sequence of images which represent the image intensity $i(x,y,t)$ in space (*i.e.*, x and y) and time t. The normalized intensity correlation function is calculated as a function of the spatial lag, ξ and η, as well as lag time, τ, by

$$r(\xi,\eta,\tau) = \langle \delta i(x,y,t)\delta i(x+\xi,y+\eta,t+\tau)\rangle_{x,y,t}, \tag{S1}$$

where $\langle\cdot\rangle_{x,y,t}$ indicates averaging over all x, y, and t, and

$$\delta i(x,y,t) = \big(i(x,y,t) - \langle i\rangle_{x,y}\big)/\langle i\rangle_{x,y}. \tag{S2}$$

To minimize computation time, $r(\xi,\eta,\tau)$ is calculated using the Fourier method.[1]

Step B

As typical in ICS analysis[1,2], for each τ, the spatial correlation function is taken to be a Gaussian of the form:

$$r(\xi,\eta) = g \times \exp\left[-\frac{(\xi-\xi_0)^2+(\eta-\eta_0)^2}{d_0^2}\right] + g_\infty, \tag{S3}$$

where the physical significance of g, ξ_0, η_0, d_0, and g_∞ are described in the main article. This spatial fitting is typically done in the least square manner, only for the central correlation area (small ξ and η), and with zero weighting for the central point ($\xi = \eta = 0$), where there is white noise contribution. We found that the optimum fit is obtained by including data points where ξ and η are smaller than 5–6 times the Gaussian width d_0. The output of this step is $g(\tau)$.

Step C

For three-dimensional (3D) Gaussian intensity profile of the excitation volume, the functional form of the temporal correlation function for a system with 3D diffusion is[3]

$$g(\tau) = g_0\left(1+\frac{\tau}{\tau_{D,xy}}\right)^{-1}\left(1+\frac{\tau}{\tau_{D,z}}\right)^{-1/2}, \tag{S4}$$

where the translational diffusion relaxation times, τ_D, in the lateral and axial directions are related to the diffusion coefficient, D, respectively, by $\tau_{D,xy} = \omega_{xy}^2/4D$ and $\tau_{D,z} = \omega_z^2/4D$. Eq. (S4) can thus be rewritten as

$$g(\tau) = g_0\left(1+\frac{4D\tau}{\omega_{xy}^2}\right)^{-1}\left(1+\frac{4D\tau}{\omega_z^2}\right)^{-1/2}. \tag{S5}$$

If one assumes that the local effective D can be related to the MSD of the probe particles, $\langle\Delta r^2(\tau)\rangle$, by $\langle\Delta r^2(\tau)\rangle = 6D\tau$, then Eq. (S5) becomes

$$g(\tau) = g_0\left(1+\frac{2\langle\Delta r^2(\tau)\rangle}{3\omega_{xy}^2}\right)^{-1}\left(1+\frac{2\langle\Delta r^2(\tau)\rangle}{3\omega_z^2}\right)^{-1/2}. \tag{S6}$$

Therefore, by solving Eq. (S6), one can obtain the MSD data from the temporal correlation function.

Step D

The logarithmic derivative of $\langle \Delta r^2(\tau) \rangle$ with respect to time is calculated as

$$\alpha(\tau) = \frac{d \ln\langle \Delta r^2(\tau) \rangle}{d \ln \tau}. \quad \text{(S7)}$$

Numerical derivation in this process typically uses Gaussian sliding window approach[4], which inherently involve smoothing of the $\langle \Delta r^2(\tau) \rangle$ data, to reduce high-frequency noise in the data. This step is not needed for the method we propose (which requires only Steps E, which improves the quality of the extracted results).

Step E

One can, in principle, directly calculate $G^{'}(\omega)$ and $G''(\omega)$ from the $\langle \Delta r^2(\tau) \rangle$ and $\alpha(\tau)$ data obtained in Steps C and D. However, the use of such an approach could lead to propagation of experimental and data processing errors arising from Step B and the Eqs. (S6) and (S7). In Step E here, we propose an alternative method that minimizes these errors.

Since $g(\tau)$, $\langle \Delta r^2(\tau) \rangle$, and $\alpha(\tau)$ are dependent on each other (as mathematically described in Eqs. (S6) and (S7)), we use an approach that eliminates the need for Eq. (S7) and determines $\alpha(\tau)$ directly from $g(\tau)$, by choosing a robust functional form for $\alpha(\tau)$, writing $\langle \Delta r^2(\tau) \rangle$ in terms of $\alpha(\tau)$, and substituting in Eq. (S6). We choose

$$\alpha(\tau) = a + b \times \mathrm{erf}[\gamma \ln(\tau/\tau_{tr})] \quad \text{(S8)}$$

and determine the parameters in Eq. (S8) by a statistical analysis of the raw $g(\tau)$ data (from Step B). The functional form in Eq. (S8) has the advantage of being able to describe asymptotic power laws and the transitions, which are prevalent in many viscoelastic materials, as stated in the main article.

Step F

The $\langle \Delta r^2(\tau) \rangle$ and $\alpha(\tau)$ data obtained from Step E can then be used to calculate the frequency-dependent storage modulus, $G^{'}(\omega)$, and loss modulus, $G''(\omega)$, from

$$G'(\omega) + iG''(\omega) = \frac{n k_B T}{3\pi a \langle \Delta r^2(\omega) \rangle \Gamma[1+\alpha(\omega)]} \left(\cos\left[\frac{\pi \alpha(\omega)}{2}\right] + i \sin\left[\frac{\pi \alpha(\omega)}{2}\right] \right). \quad \text{(S9)}$$

Step G

In addition to the microrheological information obtained in the previous steps, a number of 'standard' ICS measurements can also be obtained from the spatiotemporal correlation function $r(\xi, \eta, \tau)$. The methods to obtain this information can be found in the ICS literature, which has been extensively reviewed by Kolin and Wiseman.[5]

Illustrations

To illustrate the usefulness of Step E, we show one typical extracted result based on this procedure and compare it to the result obtained from a combination of Steps C and D, for the raw $g(\tau)$ data (Fig. S2), the $\langle \Delta r^2(\tau) \rangle$ data (Fig. S3), as well as the $G'(\omega)$ and $G''(\omega)$ data (Fig. S4).

Finally, we compare the ICS-μR results for complex, viscoelastic materials (PEO solutions of different concentrations) with results obtained using mechanical rheology in Fig. S5. Note that as the material becomes increasingly liquid-like at low frequency, both the magnitude and quality of the G' data decrease rapidly. For that reason and because of the logarithmic scale used in the *y*-axis, the error bar grows in size and the deviation between the results from the two methods may mistakenly seem to grow.

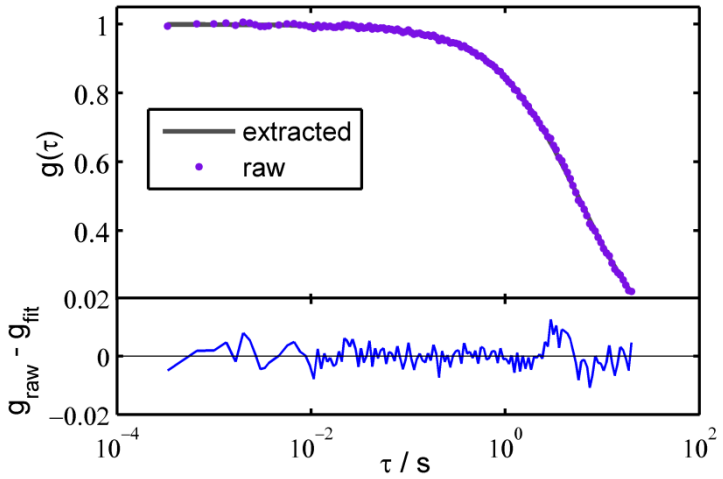

Fig. S2 Comparison between the raw, unsmoothed $g(\tau)$ data obtained from Step B and the extracted $g(\tau)$ data obtained from Step E. The bottom panel shows the difference between the two data sets.

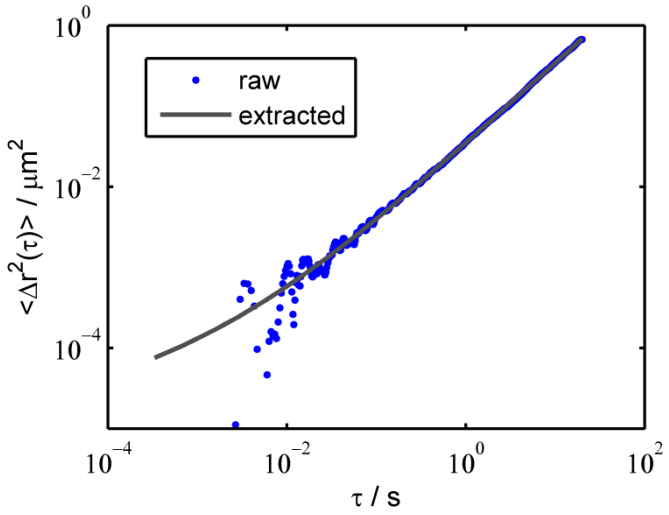

Fig. S3 Comparison between the $\langle \Delta r^2(\tau) \rangle$ data obtained from Step C and the extracted $\langle \Delta r^2(\tau) \rangle$ data obtained from Step E. Note the data truncation in the raw data at small τ due to amplified carry-over noise from the raw $g(\tau)$ data in Step B.

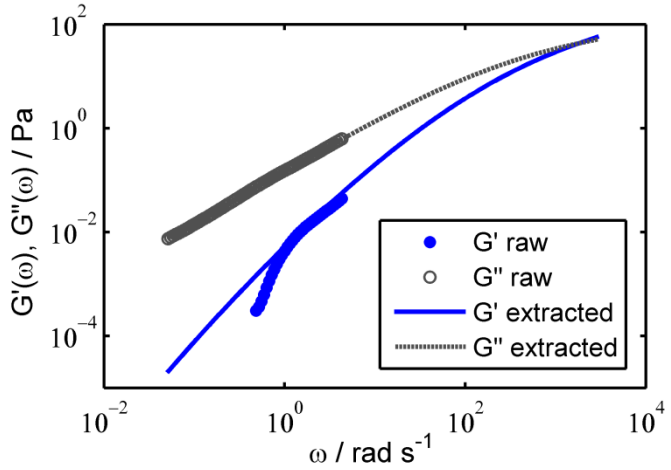

Fig. S4 Comparison between the 'raw' $G^{'}(\omega)$ and $G''(\omega)$ data obtained from Steps C, D, and F and the extracted $G^{'}(\omega)$ and $G''(\omega)$ data obtained from Steps E and F. The noise in the raw $g(\tau)$ data (Fig. S2) is doubly amplified through calculation of $\langle \Delta r^2(\tau) \rangle$ in Step C (Fig. S3) and $\alpha(\tau)$ in Step D, forcing severe data truncations in the 'raw' $G^{'}(\omega)$ and $G''(\omega)$ data.

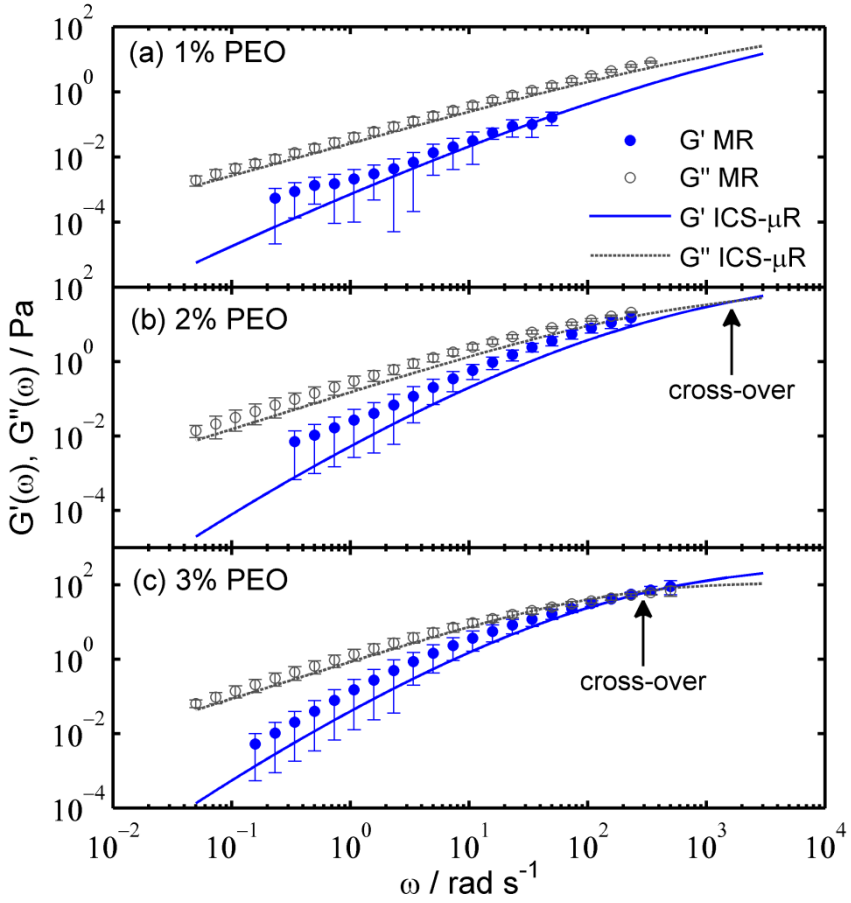

Fig. S5 Comparison between frequency-dependent linear viscoelastic moduli for PEO aqueous solutions of various concentrations as measured with ICS-μR and mechanical rheometer (MR). ICS-μR results were obtained from $\langle \Delta r^2(\tau) \rangle$ of 0.5 μm beads in the solutions. The error bars signify the extent of experimental error in the mechanical rheology measurement.

References

1. M. Srivastava and N. O. Petersen, *Methods Cell Sci.*, 1996, **14**, 47-54.
2. P. W. Wiseman, J. A. Squier, M. H. Ellisman and K. R. Wilson, *J. Microsc.*, 2000, **200**, 14-25.
3. S. R. Aragón and R. Pecora, *J. Chem. Phys.*, 1976, **64**, 1791-1803.
4. B. R. Dasgupta, S.-Y. Tee, J. C. Crocker, B. J. Frisken and D. A. Weitz, *Phys. Rev. E,* 2002, **65**, 051505.
5. D. L. Kolin and P. W. Wiseman, *Cell Biochem. Biophys.*, 2007, **49**, 141-164.